AIAA 81-4167

Effect of Acceleration Switching During INS In-Flight Alignment

Boaz Porat*
Stanford University, Stanford, Calif.
and
Itzhack Y. Bar-Itzhack†
Technion—Israel Institute of Technology, Haifa, Israel

Covariance simulation results are presented that show that the application of alternating axial acceleration to inertial navigation systems (INS) during planar in-flight alignment (IFA) results in an alignment time that is longer than that produced by a constant axial acceleration. Similarly, an S-shaped maneuver, which by its nature requires acceleration sign changes, yields a longer alignment time than that produced by a circular flight path. These results are also obtained analytically when simple IFA models, developed in an earlier work, are used. Using the simple models it is shown that acceleration sign changes produce a correlation coefficient between the measured INS velocity error and the azimuth misalignment angle that crosses zero. This finding yields the explanation to the phenomenon of increased alignment time when the acceleration changes sign during the IFA.

I. Introduction

In a recent work[1] the problem of in-flight alignment (IFA) of an inertial navigation system (INS) was investigated. That work dealt with the issue of azimuth observability enhancement that was accomplished by subjecting the INS to accelerations generated by maneuvers of a combat aircraft. In particular, that work investigated the difference between the influence of axial and lateral accelerations on the azimuth observability during IFA.

It was found that, observing the IFA achievements at the end of the maneuver, axial maneuvers are not, in general, superior to lateral ones. There are, however, three classes of alignment problems in which axial maneuvers are superior. Moreover, since the azimuth alignment problem in these classes is a planar one, a simple analytic model was found that described very well the INS behavior in azimuth during the IFA maneuvers. When the azimuth gyro constant drift rate is small, the model is a third-order one while if that drift is not small, the model is a fourth-order one. These results were verified through covariance simulations of the full order INS error model.

The two characteristic maneuvers that were analyzed in Ref. 1 and for which these conclusions were derived were: a circular maneuver that represented the cases in which lateral accelerations are applied, and a constant axial acceleration maneuver that represented the cases in which axial accelerations are applied. While a circular maneuver is a realistic one, the pilot may prefer to perform S-shaped turns, specially when a reduction in flight time is desired. On the other hand, a constant axial acceleration for the duration necessary for the alignment is not attainable. A more realistic axial maneuver then is an alternating acceleration maneuver.

In this work we investigate the INS azimuth behavior during IFA when S-shaped turns and an alternating axial acceleration maneuver are performed. As in Ref. 1, the investigation is carried out only for the three classes of alignment problems in which the azimuth alignment is a planar problem.

The reason for the particular attention given to these maneuvers is that although the general conclusions drawn in Ref. 1 concerning the difference between the influence of lateral and axial maneuvers on the INS azimuth behavior still hold, the effect of these two maneuvers differ from that of the maneuvers analyzed in Ref. 1 in an unexpected and rather interesting way.

In the next section simulation results will be presented that will demonstrate the effect of S-shaped maneuver and alternating axial acceleration maneuver on the INS azimuth behavior. In Sec. III analytic results obtained from the simple models will be derived, and then in Sec. IV an explanation to the peculiar effect these two maneuvers have will be suggested.

II. Simulation Results

First we wish to illustrate that the conclusion of Ref. 1, concerning the superiority of axial acceleration when the IFA problem is a planar one, still hold. For an example we turn to Figs. 1 and 2. These plots are the result of a covariance simulation in which the lateral acceleration is represented by the acceleration generated on an S-shaped trajectory whereas the axial acceleration is an alternating axial acceleration. The mathematical description of the first maneuver is given by

$$a_N(t) = -A \cdot \sin\omega t \cdot \text{sign}(\cos\omega t) \qquad a_E(t) = A \cdot \cos\omega t \quad (1)$$

and that of the second one is given by

$$a_N(t) = -A \cdot \text{sign}(\cos\omega t) \qquad a_E(t) = 0 \quad (2)$$

where $a_N(t)$ is the north component of the aircraft acceleration and $a_E(t)$ is the east component. The time history of the acceleration vectors during these maneuvers is shown in Fig. 3. Note that for fair comparison, all accelerations have equal magnitude. The switching instants of the axial acceleration are chosen to coincide with those of the lateral acceleration. The values used in the simulation are those used in Ref. 1.

More intriguing differences, though, are the difference between the effect of a constant acceleration and that of an alternating axial acceleration and the difference between the effect of a circular and that of an S-shaped trajectory. Figure 4 demonstrates the difference between the effect of the two axial accelerations, and Fig. 5 demonstrates the difference between the effects of the two lateral accelerations. All four plots are the results of covariance simulations of case I of Ref. 1 in which the major error source is the azimuth misalignment.

Received Jan. 29, 1980; revision received Aug. 15, 1980.

*Graduate Student, Department of Electrical Engineering.
†Associate Professor, Department of Aeronautical Engineering.

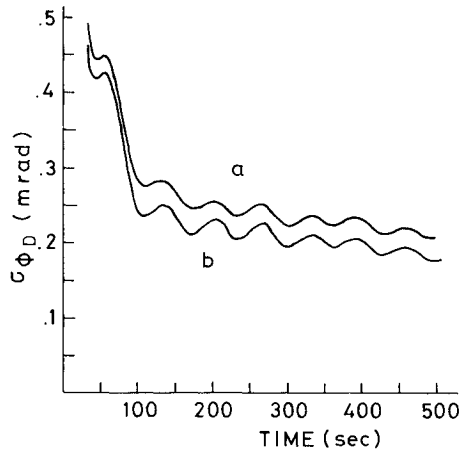

Fig. 1 Standard deviation of the azimuth misalignment estimation error derived from the simulation of case II: a) for S-shaped trajectory, b) for alternating axial acceleration.

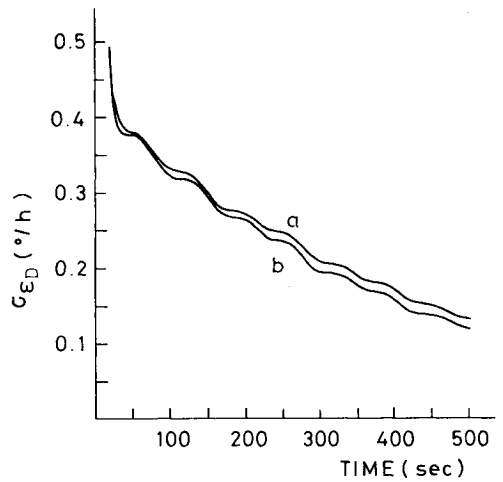

Fig. 2 Standard deviation of the azimuth gyro drift rate estimation error derived from the simulation of case II: a) for S-shaped trajectory, b) for alternating axial acceleration.

The interesting effect seen in both Fig. 4 and Fig. 5 is that constant axial acceleration is superior to alternating axial acceleration and that circular trajectory is superior to an S-shaped trajectory.

A similar effect takes place when the drift rate of the azimuth gyro is not negligible. This can be seen in Figs. 6-9.

We observe that when acceleration switching takes place during the IFA (i.e., when alternating axial acceleration is applied or when an S-shaped trajectory is flown) the estimation is impaired. When only azimuth misalignment is present the estimation of this error is temporarily halted after the switching instant. When both azimuth misalignment and azimuth gyro drift rate are present, the estimation of the constant drift rate as well as that of the azimuth misalignment is temporarily halted after the switching instant; thus the standard deviation of the azimuth misalignment estimation error starts growing until the estimation process resumes.

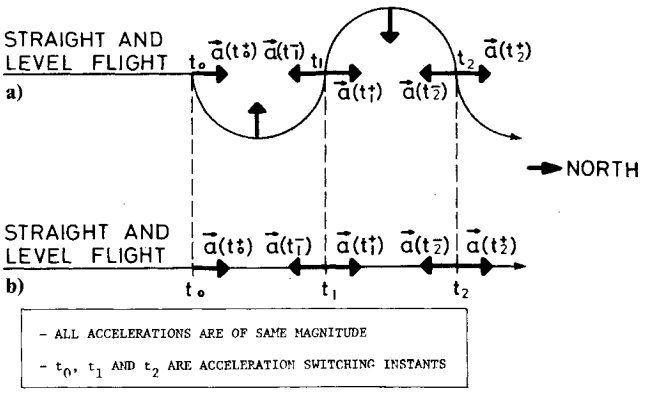

Fig. 3 Acceleration vector time histories during IFA: a) for S-shaped trajectory, b) for alternating axial acceleration.

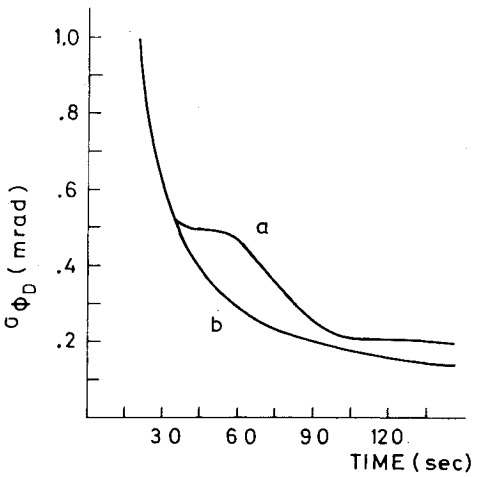

Fig. 4 Standard deviation of the azimuth misalignment estimation error derived from the simulation of case I: a) for alternating axial acceleration, b) for constant axial acceleration.

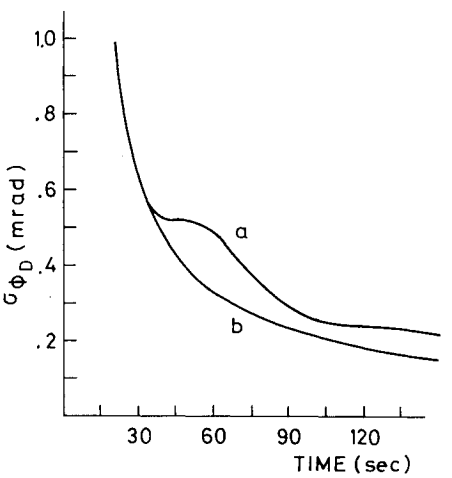

Fig. 5 Standard deviation of the azimuth misalignment estimation error derived from the simulation of case I: a) for S-shaped maneuver, b) for circular maneuver.

III. Analytic Results

The simulation results presented in the preceding section were of a *planar* IFA problem. In Ref. 1 an IFA planar problem was defined as an IFA of an INS whose dominant errors are azimuth misalignment and/or azimuth gyro drift rate. It was shown there that a planar IFA problem can be modeled by a simple third- or fourth-order linear model. We now pose the following question: Do the analytic models yield the difference between the continuous acceleration IFA and the switched acceleration IFA which were observed in the simulations and presented in the preceding section?

To answer this question we assume, for simplicity, that the acceleration is switched only once, for if the analytic models describe the difference between the continuous and switched cases after just one switch, they surely match the simulation for the rest of the IFA.

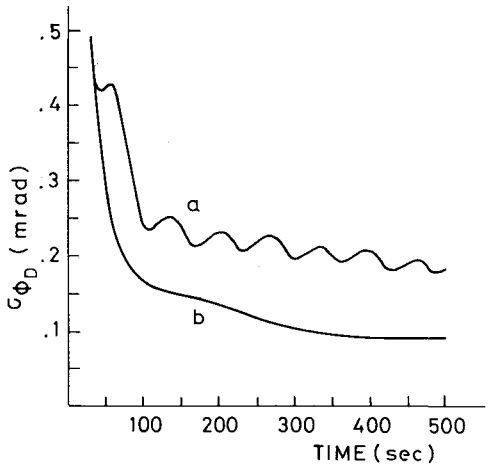

Fig. 6 Standard deviation of the azimuth misalignment estimation error derived from the simulation of case II: a) for alternating axial acceleration, b) for constant axial acceleration.

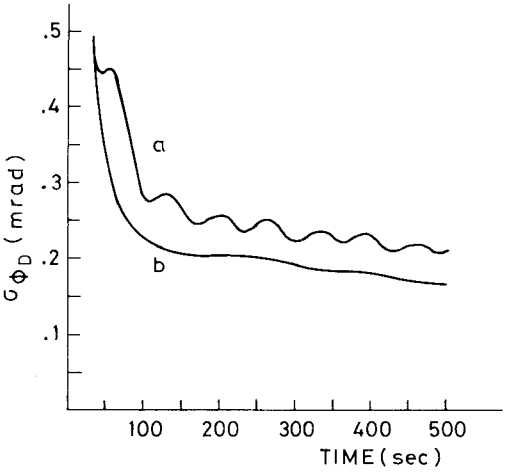

Fig. 8 Standard deviation of the azimuth misalignment estimation error derived from the simulation of case II: a) for S-shaped trajectory, b) for circular trajectory.

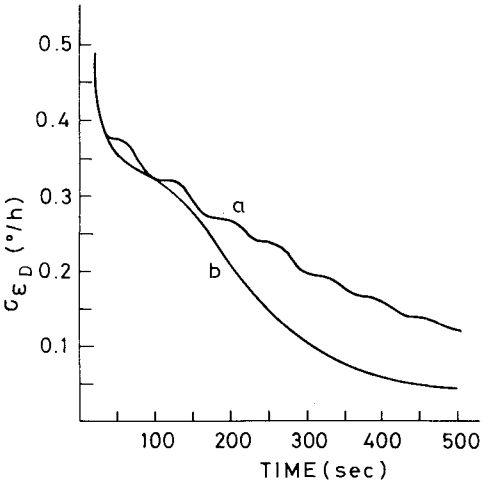

Fig. 7 Standard deviation of the azimuth gyro constant drift rate estimation error derived from the simulation of case II: a) for alternating axial acceleration, b) for constant axial acceleration.

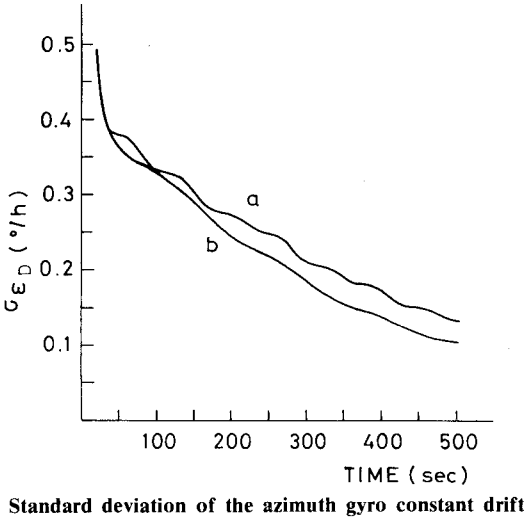

Fig. 9 Standard deviation of the azimuth gyro constant drift rate estimation error derived from the simulation of case II: a) for S-shaped trajectory, b) for circular trajectory.

A. Third-Order Model—Axial Acceleration

As in Ref. 1 we assume that at the beginning of the accelerated part of the IFA the aircraft accelerates at a constant acceleration A, due north. Using the model developed in Ref. 1 the value of P^{-1} can be computed at any time and in particular at the switching instant t_0 where A is replaced by $-A$. To find the value of P^{-1} at any time t larger than t_0 we use[2]

$$P^{-1}(t) = \Psi^T(t_0,t)P^{-1}(t_0)\Psi(t_0,t) + \int_{t_0}^{t} \Psi^T(\tau,t)H^T R^{-1} H \Psi(\tau,t)\,d\tau \qquad (3)$$

where $\Psi(b,a)$ is the transition matrix that transforms the state vector of the autonomous system from time a to time b. After evaluating $P^{-1}(t_0)$, using Eq. (28) of Ref. 1, $P^{-1}(t)$ can be computed using Eq. (3). The inversion of the resulting matrix yields

$$\sigma^2_{\phi_D}(t) = 12\frac{\sigma_v^2}{A^2}\left[t^3 - 12\frac{t_0^2(t-t_0)^2}{t}\right]^{-1} \qquad (4)$$

whereas if no switching takes place[1]

$$\sigma^2_{\phi_D}(t) = 12\frac{\sigma_v^2}{A^2}\frac{1}{t^3} \qquad (5)$$

Obviously the acceleration switch from A to $-A$ at t_0 impairs the estimation of ϕ_D. From Eqs. (4) and (5) it can be seen that when $t \approx t_0$ or when $t \gg t_0$ the switching effect is negligible but when $t \approx 2t_0$, which is, approximately, the time at which the second acceleration switch takes place, the relative difference is significant. Figure 10 illustrates the difference between σ_{ϕ_D} obtained from the analytic model when the axial acceleration is constant all the way, and σ_{ϕ_D} when the constant acceleration changes sign at t_0.

B. Third-Order Model—Lateral Acceleration

Up to a quarter of a circle the S-shaped maneuver matches the circular maneuver; that is,

$$a_N(t) = -A\cdot\sin\omega t \qquad a_E(t) = A\cdot\cos\omega t \qquad (6)$$

where $a_N(t)$ is the north component of the acceleration and $a_E(t)$ is the east component. After a quarter of a circle; that is, when $\omega t = \omega t_0 = \pi/2$ the north component of the acceleration changes sign such that for $t > t_0$

$$a_N(t) = A\cdot\sin\omega t \qquad a_E(t) = A\cdot\cos\omega t \qquad (7)$$

Using Eq. (20) of Ref. 1 to compute $P^{-1}(t_0)$ where $t_0 = \pi/2\omega$ and then using Eq. (3), the following expression is obtained

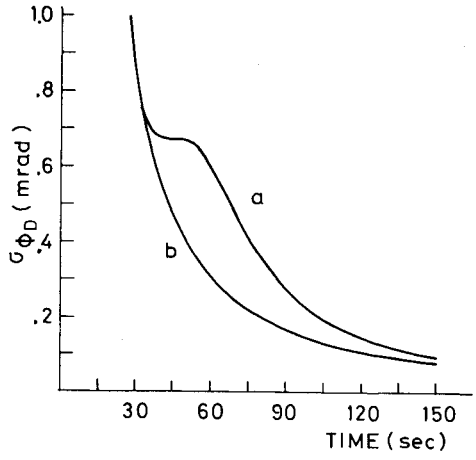

Fig. 10 Standard deviation of the azimuth misalignment estimation error derived from the third-order analytic model: a) for axial acceleration with one acceleration switch, b) for constant axial acceleration.

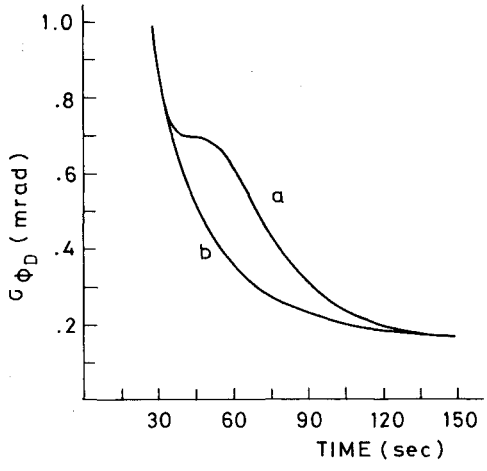

Fig. 11 Standard deviation of the azimuth misalignment estimation error derived from the third-order analytic model: a) for lateral acceleration with one acceleration switch, b) for circular maneuver.

$$\sigma^2_{\phi_D} = \frac{\omega^3 \sigma_v^2}{A^2} \frac{\omega t}{(\omega t)^2 + 2\cos\omega t + 4\sin\omega t - 6} \tag{8}$$

If now after each completion of a semicircle (beyond t_0) the sign of $a_N(t)$ changes, an S-shaped trajectory is obtained. However, as stated before, we analyze the difference between the continuous (circular) and switched (S-shaped) cases after just one switch. If no switching takes place then[1]

$$\sigma^2_{\phi_D} = \frac{\omega^3 \sigma_v^2}{A^2} \frac{\omega t}{(\omega t)^2 - 2(1 - \cos\omega t)} \tag{9}$$

Note from Eqs. (8) and (9) that, as expected, when $t = \pi/2\omega$ both cases yield the same result and that for large t in both cases $\sigma^2_{\phi_D}$ decreases as $1/t$. As $\sin\omega t \leq 1$ it can be easily shown that

$$(\omega t)^2 + 2\cos\omega t + 4\sin\omega t - 6 \leq (\omega t)^2 - 2(1 - \cos\omega t) \tag{10}$$

We therefore conclude that apart from discrete isolated instants, σ_{ϕ_D} of the continuous case is smaller than that of the switched case.

We use Eqs. (8) and (9) to plot in Fig. 11 the difference between σ_{ϕ_D} obtained from the analytic model when the aircraft performs a circular maneuver, and the σ_{ϕ_D} obtained

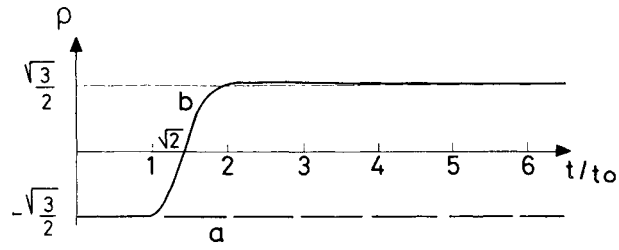

Fig. 12 Plots of $\rho(t/t_0)$ for a) constant continuous axial acceleration and b) constant axial acceleration switched at t_0.

when one acceleration switch occurs at $t_0 = \pi/2\omega$. Similar results can be obtained using the fourth-order model that demonstrates that the behavior of σ_{ϕ_D} and σ_{ϵ_D} in the simulation can be obtained from the analytic model. The development, though, is cumbersome and the expressions obtained are not too instructive; therefore, we choose not to present them here.

IV. Analysis

We have seen so far that acceleration sign changes reduce the stochastic observability of the azimuth gyro constant drift rate and of the azimuth misalignment. We have also seen that the analytic models developed in Ref. 1 do indeed confirm this phenomenon. We now wish to find an explanation to it. To meet this end we analyze the thrid-order model and we consider only axial accelerations. We choose this combination because it is the simplest one. The conclusions drawn from this simple analysis can be extended to the rest of the cases.

It can be shown[1] that when the IFA problem can be modeled by a third-order model, P takes the following form:

$$P = \begin{bmatrix} \sigma^2_{v_N} & 0 & 0 \\ 0 & \sigma^2_{v_E} & \rho\sigma_{v_E}\sigma_{\phi_D} \\ 0 & \rho\sigma_{v_E}\sigma_{\phi_D} & \sigma^2_{\phi_D} \end{bmatrix} \tag{11}$$

while, the dynamics matrix takes the form

$$F = \begin{bmatrix} 0 & 0 & 0 \\ 0 & 0 & -a_N(t) \\ 0 & 0 & 0 \end{bmatrix} \tag{12}$$

As stated before, we assume, with no loss of generality, that the axial acceleration is due north. The estimation error covariance matrix P develops according to[3]

$$\dot{P} = FP + PF^T - PH^T R^{-1} HP \tag{13}$$

which, using the special forms of P and F given in Eqs. (11) and (12), respectively, yields

$$\frac{\mathrm{d}}{\mathrm{d}t}(\sigma^2_{\phi_D}) = -\frac{1}{\sigma_v^2}(\rho\sigma_{v_E}\sigma_{\phi_D})^2 \tag{14}$$

Using separation of variables, Eq. (14) can be easily solved to yield

$$\sigma^2_{\phi_D}(t) = \sigma^2_{\phi_D}(0)\exp\left\{-\frac{1}{\sigma_v^2}\int_0^t \rho^2(\tau)\sigma^2_{v_E}(\tau)\mathrm{d}\tau\right\} \tag{15}$$

From Eq. (28) of Ref. 1 it can be shown that when $a_N(t) = A$, where A is constant, and when there is no sign change, then

$$\rho(t) = -\sqrt{3}/2 \tag{16}$$

From the analysis of the preceding section it can be shown that when at t_0 $a_N(t)$ changes direction such that for $t > t_0$

$a_N(t) = -A$, then

$$\rho(t) = -\frac{t_0^2 - \frac{1}{2}t^2}{(\frac{1}{3}t^4 - 2t_0^2t^2 + 2t_0^3t)^{\frac{1}{2}}} \tag{17}$$

The value of ρ is plotted in Fig. 12 for both cases where the time is normalized to the switching instant t_0.

The shape of $\rho(t)$ and the role $\rho(t)$ plays in Eq. (15) yields an explanation to the fact that when the aircraft acceleration changes sign, the observability of ϕ_D decreases; namely, in zones where $\rho(t)$ and thus $\rho^2(t)$ are approximately zero, the value of the integral in Eq. (15) does not increase and thus $\sigma_{\phi_D}(t)$ in this time increment does not decrease; that is, the estimation process in being halted. If this is the only sign change, then after a long time the effect of this zone on the integral diminishes and the estimation errors in the continuous and the switched acceleration IFA approach the same value. If the switching occurs repeatedly then each time $\rho(t) \approx 0$ a halt in the estimation process takes place.

V. Conclusions

It is well known that in order to enhance the azimuth alignment and calibration of an inertial navigation system (INS) during in-flight alignment (IFA) an acceleration vector not collinear with g has to be applied. It is intuitively felt that the better this vector spans the two dimensional space perpendicular to the gravity vector, the faster the azimuth alignment and calibration process. Therefore, after having seen in Ref. 1 the influence of IFA maneuvers on the azimuth estimation, one would expect that reversing of the constant axial acceleration will shorten the azimuth alignment process. Similarly one would expect that an S-shaped maneuver yields an azimuth alignment process that is faster than that obtained by a circular maneuver. It was shown in this work that simulation results contradict these expectations. It was also shown that the simple third- and fourth-order linear models of Ref. 1 yield the same results; thus it is concluded that this phenomenon is not a marginal one but rather *a main feature* of the azimuth estimation process. It was shown in this work that when an acceleration reversal takes place, the correlation coefficient, that correlates the measured velocity error and the azimuth misalignment, changes sign and thus crosses zero which temporarily halts the estimation process. This, in fact, explains also the results obtained in Ref. 1; namely, the fact that when the IFA problem is a planar one, axial acceleration is superior to the acceleration generated on a circular trajectory. The rationale is that an abrupt reversal of the axial acceleration that was considered in the present work is replaced, on a circular trajectory, by a gradual reversal of the direction of the applied acceleration. Thus the estimation rate on a circular trajectory stands somewhere between the estimation rate of a constant axial acceleration path and that of an alternating acceleration path.

References

[1] Bar-Itzhack, I.Y., and Porat, B., "Azimuth Observability Enhancement During INS In-Flight Alignment," *Journal of Guidance and Control,* Vol. 3, July-Aug. 1980, pp. 337-344.

[2] Bryson, A.E. Jr. and Ho, Y.C., *Applied Optimal Control,* Blaisdell Publishing Co., Waltham, Mass., 1969, p. 370.

[3] Gelb, A., *Applied Optimal Estimation,* MIT Press, Cambridge, Mass., 1974, p. 122.